

reprinted from:

# **TEMPERATURE**

**ITS MEASUREMENT  
AND CONTROL  
IN SCIENCE AND INDUSTRY**

**VOLUME FIVE  
PART TWO**

**Thermal response times of some  
cryogenic thermometers**

D. Linenberger, E. Spellicy, and R. Radebaugh

**AIP**

Published by American Institute of Physics

# Thermal response times of some cryogenic thermometers<sup>a,b</sup>

D. Linenberger, E. Spellicy, and R. Radebaugh

*Thermophysical Properties Division, National Bureau of Standards, Boulder, Colorado 80303*

The measurement of time-varying temperatures requires sensors with sufficiently fast response times. As an aid to the selection of a satisfactory thermometer, this paper describes the measurement of the thermal time constants of several cryogenic thermometers. The thermal time constants were measured by observing the response of the thermometers to self-heating induced by the injection of a constant current step. Temperatures studied were 4, 77, and 295 K. Measurements were made in both the gas and liquid phases of helium and nitrogen in order to determine the upper and lower limits of the time constants. Specific thermometers investigated include a germanium resistance thermometer, carbon resistors, diodes, and a silicon-on-sapphire resistance device (area  $\sim 0.35 \text{ mm}^2$ ). In several cases the measurements are compared with the calculated values of the time constants.

## INTRODUCTION

Many applications in thermometry require that the characteristic time response of a particular thermometer be known to determine its suitability in a measurement task. The purpose of this paper is to describe a simple method for the determination of the thermal time constant  $\tau$  of some common cryogenic thermometers. Also presented are typical values of  $\tau$  for a variety of such devices, at temperatures of 4 K, 76 K, and 295 K. A theoretical treatment based on known thermal properties of the thermometers is given as a basis of interpretation of our results.

The thermal time constant of any thermometer is strongly dependent on the particular mounting arrangement used to provide heat transfer and on the surrounding medium. This paper addresses some of these questions and gives results which would be applicable to a variety of environments. If accurate time constants are required, then it would be necessary to measure them *in situ*. This paper describes a method of *in situ* measurement. One common thermometer not measured in this work was the thermocouple since it does require a different and more sophisticated measurement technique.<sup>1</sup>

## MEASUREMENT TECHNIQUE

The measurement apparatus is based upon the Wheatstone bridge circuits<sup>2</sup> shown in Figure 1. With an applied dc voltage across the E terminals, we note that the thermometer resistance  $R_t$  is determined to be the same as the nulling resistance  $R_n$  which sets V equal to zero. In our apparatus,  $R_n$  was a precision decade resistor and V was monitored by a sensitive digital voltmeter. In Figure 1a, the bridge resistors R were equal in value, and they were of high wattage rating to avoid their changing resistance due to heating. For the actual transient measurement, a pulse generator was inserted in place of the dc voltage, giving a voltage difference  $\Delta E = E_2 - E_1$ . In this configuration, the  $E_1$  voltage ( $E_1 > 0$ ) still causes the bridge to null and gives an insignificant Joule heating to the thermometer. On the other hand,  $E_2$  is designed to give an associated change in sensor resistance due to Joule heating. The null voltage is then quantified by

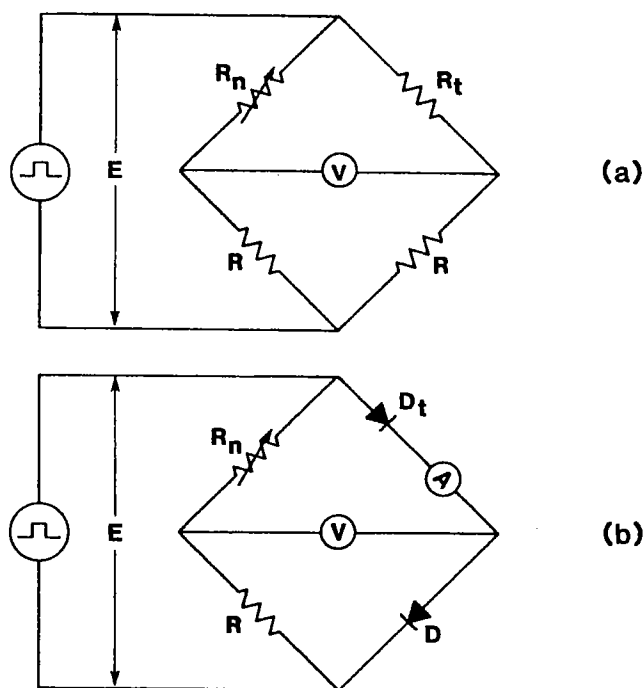


Figure 1. a) Bridge network used in determination of  $\tau$  for resistance-type thermometers. b) Bridge network used in determination of  $\tau$  for silicon diode-type thermometers.

$$V = \frac{(R_n - R_t)R}{(R + R_n)(R + R_t)} E \quad (1)$$

The voltage  $E_2$  was chosen such that the temperature rise  $\Delta T$  of the thermometer was about 10% of the absolute temperature. Such a value gave a good sensitivity but yet the temperature change was still small

enough to keep on a locally linear portion of the R versus T curve and to keep the thermal properties from changing significantly. The  $\Delta T$  was determined from the known R versus T characteristic of the thermometer. The R value of the heated resistor was found by adjusting  $R_h$  to null the bridge with the dc voltage  $E_2$  applied. The power dissipated by the resistance thermometer is given by

$$P = E^2 R_t / (R + R_t)^2 \quad (2)$$

Figure 1b shows a modified Wheatstone bridge arrangement used for the measurement of the  $\tau$  values of various diode thermometers. The principles and procedures that govern the use of resistive-base Wheatstone bridge techniques are in general applicable to diode thermometers. The modifications are: (1) The diode thermometer  $D_t$  is placed in series with ammeter A. The ammeter and a sensitive voltmeter placed across the diode (not shown) are used to determine the power input into the diode. (2) A diode D replaces the resistor on one of the bridge arms. Note that for a forward biased diode, the forward current is related to the voltage in a generally exponential way, therefore, the resistance of the diode varies similarly. The purpose of the diode is to track (thus approximately canceling) the electrically (non-heating) induced resistive changes in  $D_t$  as the current through the diodes is increased. (3) The value of R is non-critical for considerations of bridge sensitivity. We chose R approximately equal to the on-resistance of D (via ohmmeter).

A digital oscilloscope with selectable sampling rates of up to 2  $\mu$ s/data point captured the V transient waveform and was used to process the waveforms. The E waveform was also recorded to fix both the pulse onset and power into the thermometer. (Pulse period  $\geq 1$  s at  $\sim 25\%$  duty cycle.) Typical V waveforms are shown in the upper curves of Figure 2 (resistive thermometer) and Figure 3 (diode thermometer). If one were observing a first-order system (a thermometer of homogeneous construction and the addenda completely isolated), one could get an approximate  $\tau$  value by observing the time on these curves where the exponential response experiences a  $[1 - \exp(t/\tau)] = 0.63$  change from the initial

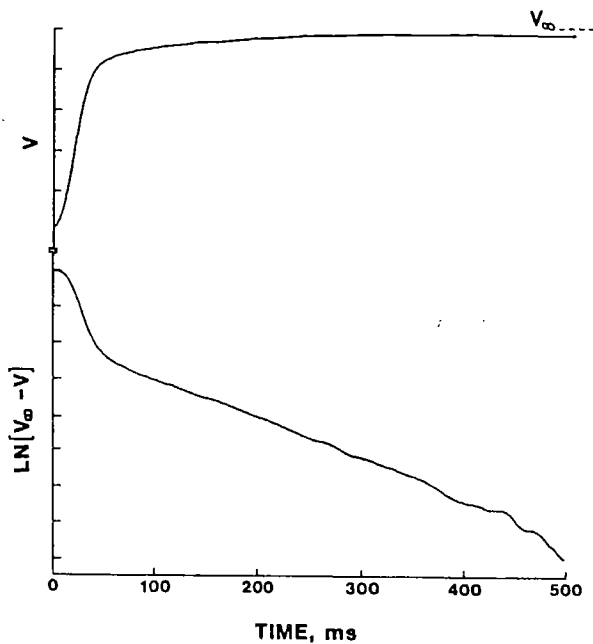


Figure 2. Upper curve is 1/8 W carbon thermometer's response to a pulse (onset at time=0s) in He gas at 4.2 K. Lower curve is the natural logarithm of the upper curve. Vertical axis calibrated in arbitrary units.

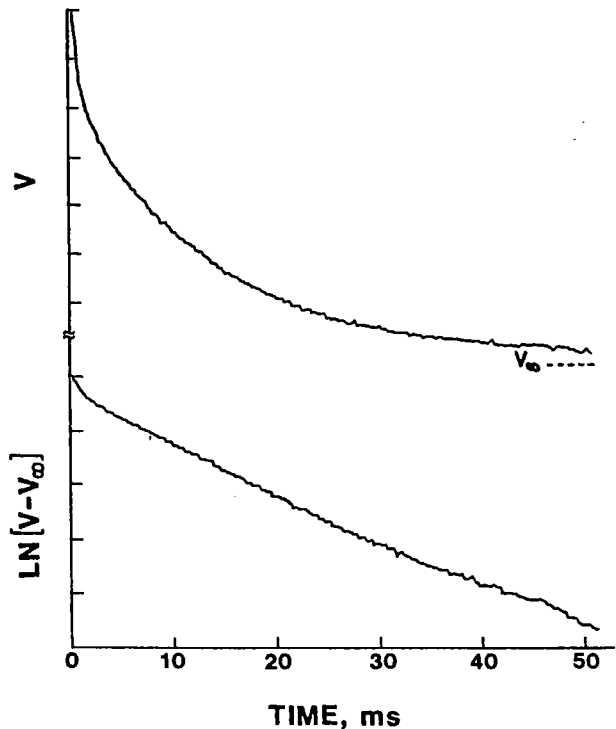


Figure 3. Upper curve is the miniature silicon-diode thermometer's response to a pulse (onset at time=0s) in He gas at 4.2 K. Lower curve is the natural logarithm of the upper curve. Vertical axis calibrated in arbitrary units.

amplitude. Unfortunately one rarely finds such one-mode thermometers useful in practice. A thorough discussion of higher-order mode behavior in thermometers is given by Kerlin et al.<sup>3,4,5</sup>

In order to get an indication of at least the simpler modes of behavior for the thermometers tested, the upper waveforms of Figures 2 and 3 were processed further. We started with the first-order expression for the bridge null voltage with the resistive-type of thermometer:

$$V(t) = V_0 + (V_\infty - V_0)(1 - e^{-t/\tau}), \quad (3)$$

where  $V_0$  is the initial voltage (usually zero) and  $V_\infty$  is the final voltage reached at time  $t \gg \tau$ . This equation describes the form of the upper curves in Figures 2 and 3. Equation 3 can be rewritten as

$$V_\infty - V(t) = (V_\infty - V_0)e^{-t/\tau} \quad (4)$$

The logarithm of this function is then

$$g(t) = \ln[V_\infty - V(t)] = \ln(V_\infty - V_0) - t/\tau, \quad (5)$$

which represents a straight line with the inverse slope equal to  $\tau$ . The lower curve of Figure 2 is  $g(t)$  (which has been smoothed digitally to some extent), but we see two distinct portions of lines, each with its characteristic slope (time constant). We discuss the significance of these slopes in the next section.

The diodes show similar behavior, except that after the initial electrical effect on V, the voltage V decreased exponentially with time as the diode heated. Thus, for diodes we used the logarithmic curve

$$g(t) = \ln[V(t) - V_\infty] = \ln(V_0 - V_\infty) - t/\tau, \quad (5a)$$

which is shown as the lower part of Figure 3, this time unsmoothed.

The thermometers were mounted on a dip probe with a two-lead electrical connection brought out to the measurement apparatus. For all sensors, a thermal time constant measurement was taken under the following conditions: immersion in liquid helium and its cold gas, immersion in liquid nitrogen and its cold gas; for some sensors, a measurement was taken in air at room temperature. No attempt was made to induce a fluid flow around the sensor. The sensor was allowed to come into thermal equilibrium with its surroundings before testing began.

In general, the time constants in liquid and gaseous cryogenics represent the two extremes associated with a particular thermometer because of the large difference in heat transfer coefficient between that in a liquid and that in a gas. In most cases the heat transfer coefficient in a liquid is high enough that the dominant thermal resistance between the thermometer and the liquid is the internal thermal resistance of the thermometer itself.

In a still gas the heat transfer coefficient is relatively small. Thus, the time constant in the gas is typical of the maximum value which would be experienced by such a thermometer in an experimental situation. Often times thermometers are used in a vacuum space and thermal contact is made by the use of an adhesive or a grease. The unit thermal conductance of a thin glue line is usually close to that for heat transfer to liquid helium or nitrogen.<sup>6,7</sup>

#### THERMOMETERS

The following is a listing of the thermometers used in our study along with pertinent aspects of their construction and experimental preparation:

**Carbon Resistors:** Carbon composition resistors provide an inexpensive thermometer with a useful range from approximately 100 K to below 1 K.<sup>8</sup> The radio-type carbon resistor consists of a cylindrical graphite with binder slug encased in a phenolic outer cylinder. Embedded in the phenolic are two opposing copper leads which make ohmic contact with the graphite. This study included three sizes with typical diameters in millimeters (parenthesis) 1/8 W (1.6), 1/4 W (2.3) and 1/2 W (3.6). All were nominally valued at 220  $\Omega$ . It has been shown that heat flow rate and thermal conductivity are independent of the electrical resistance within each size.<sup>9</sup> All resistors were suspended by their leads, which were thermally anchored 5 mm from the resistor.

Though not a thermometer per se, we also tested a loose bundle (diameter  $d \sim .5$  mm) of graphite fibers 2 cm long. Each fiber has an average diameter of 8  $\mu$ m. We felt such a structure would provide a geometrically degenerate case of the carbon resistor cylinder. Each fiber in the bundle would act as a single sensor with a typical  $\tau$ . The ends of the fiber bundle were affixed to copper mounting leads with silver paint.

**Germanium Resistance Thermometer (GRT):** In general, these devices provide very reproducible thermometry in the range  $< 100$  K. Details of construction vary by manufacturer; Halverson and Johns<sup>10</sup> provide an exposition on these practices. We selected a GRT whose construction style is typical of many in common use. A germanium sensor element ( $\sim 10$  mg) is surrounded by a Au-plated Cu enclosure ( $d \sim 3.5$  mm) with <sup>4</sup>He serving as a heat transfer medium. The two current leads were solder-contacted onto the immersion probe with the GRT freely suspended.

**Silicon-on-Sapphire Resistance Thermometer:** Figure 4 shows a schematic layout of a silicon-on-sapphire (SOS) resistance thermometer/heater used in our study.<sup>11</sup> Standard semiconductor mask and doping techniques were used to fabricate two thermometers (and device heater) with 0.7  $\mu$ m thick silicon on a 0.125 mm thick sapphire substrate.<sup>12</sup> A layer of Au was deposited upon the Al pads, upon which 6 Au wires ( $d \sim 50$   $\mu$ m) were attached with a minimum of In solder. The device was suspended

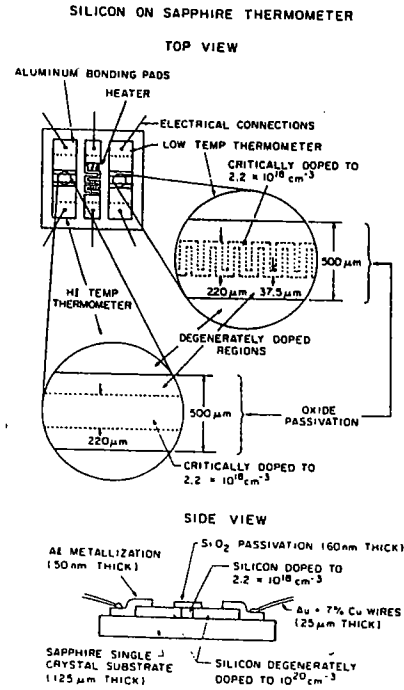


Figure 4. Drawing of silicon-on-sapphire (SOS) thermometer showing construction details. Sapphire substrate is 0.635 cm square.<sup>11</sup>

over a small machined well in the probe tip by these wires, which were glued in place  $\sim 1.5$  mm from edge of the substrate. Only the high temperature thermometer (see Fig. 4) was studied in this work, and so electrical connections were made only to that thermometer.

**Silicon diodes:** Silicon diode thermometers provide good temperature response in the range from 1 K through room temperature. The diodes tested include (1) a miniature ( $d \sim 0.5$  mm) epoxy-encapsulated device commercially produced to meet precision thermometry applications; (2) a glass-encapsulated diode ( $d \sim 1.9$  mm) used mainly in electrical-engineering work as a signal conditioner; (3) an unencapsulated (so-called beam lead) version of (2) with dimensions 700 x 225 x 90  $\mu$ m and a composition of Si on Au. Our test mount for diode (3) consisted of two 0.3 mm thick Au-plated Cu strips on a glass-epoxy base 1.5 mm thick and 1 cm long. Copper leads (0.08 mm) were soldered to the mount to provide electrical contact. Though not commonly used as thermometers, (2) and (3) were included to test the diodes size dependency of  $\tau$ .

#### RESULTS AND DISCUSSION

Measured values of  $\tau$  for all thermometers are shown in Table I. Due to space limitations within the table, room temperature measurements are presented here: for the carbon fiber, the characteristic  $\tau$  is

Table I. Typical time constants for cryogenic thermometers

Thermometer type	$\tau$ at 4.2 K (ms)		$\tau$ at 76 K (ms)	
	Liquid	Gas	Liquid	Gas
Resistance:				
Carbon				
1/8 W	6	7	113	1246
1/4 W	13	16	150	2452
1/2 W	30	31	426	3290
Carbon fiber	.001	.004	.006	.006
Germanium	32	32	360	3930
Silicon-on-sapphire	.006	.009	.910	1300
Silicon Diode:				
Miniature	6	13	62	343
Signal (encapsulated)	37	51	320	1590
Signal (unencapsulated)	.001	.001	3	14

0.008 ms; the miniature diode has a  $\tau$  of 1346 ms; and for the glass-encapsulated signal diode,  $\tau$  is equal to 4950 ms. The other thermometers are not sensitive enough to use at room temperature.

In reference to Table I, all  $\tau$  values of magnitude greater than 1 ms have an associated uncertainty of  $\pm 10\%$ . This uncertainty arises out of the distortion of the logarithmic "slopes" due to noise in the system and subsequent data smoothing. Furthermore, a value presented in Table I represents an average of several taken along inclusively greater portions of a particular slope, including some values disturbed by slope transition effects. Values of  $\tau$  which are less than 1 ms have uncertainties of  $\pm 30\%$  because of contamination of some signals by electrical effects and the limited time resolution of the digital oscilloscope.

The  $\tau$  values given in Table I are those associated with the faster of two time constants. As shown in Figure 2 the 1/8 W resistor in He gas shows a small change in response after the fast rise time has occurred. This longer time constant is presumably due to thermal coupling to the sample holder through the relatively large diameter leads of the resistor.

Published values of  $\tau$  for cryogenic thermometers are not common in literature. Halverson and Johns,<sup>10</sup> using a measurement technique different from ours, found a liquid He thermal time constant of 12 ms for a GRT of similar construction and size to ours. Their reported  $\tau$  for the same GRT in the cold gas of He was 200 ms. Blakemore<sup>13</sup> using a smaller GRT found a liquid He value of 30 ms and a gaseous He value of 200 ms; his technique also differed from ours. Our  $\tau$  value for the liquid He condition shows nearly the same result as his; while our gaseous He result differs considerably from the values given in both the above-cited reports.

Because of the complex structure and heat flow patterns in each of the thermometers tested, it is difficult to derive accurate theoretical values for the time constants based on thermal properties of the thermometer and the surrounding fluid. First it is of interest to derive the internal time constant of each of the thermometers, since this is the fastest we could expect the thermometer to respond when the heat transfer coefficient between thermometer and surrounding is very high, e.g., a liquid cryogen or high velocity gas stream. Table II lists the thermal conductivity  $k$ , specific heat per unit volume  $c_v$ , and diffusivity  $\alpha = k/c_v$  of graphite<sup>9, 14</sup> and phenolic<sup>15, 16</sup> for temperatures of 4, 10, 77, and 300 K. Dimensions for three sizes of carbon resistors are shown in Table III. We note from Table II that the diffusivity in the graphite is much larger than that in the phenolic. Thus, it can be assumed that the internal time constant of the resistors is governed almost entirely by the phenolic. In calculating the time constant associated with the phenolic, we assume it to be an infinite plate of thickness  $t$  where one side is subjected to a step function in temperature. According to Jakob<sup>17</sup> the other side reaches 53% of the step change in the time

Table II. Thermal properties of carbon resistors

T (K)	Graphite			Phenolic		
	k (mW/cm·K)	$c_v$ (MJ/cm <sup>3</sup> ·K)	$\alpha$ (cm <sup>2</sup> /s)	k (mW/cm·K)	$c_v$ (MJ/cm <sup>3</sup> ·K)	$\alpha$ (cm <sup>2</sup> /s)
4	0.30	0.33	0.91	0.10	1.7	0.059
10	1.3	2.5	0.52	0.33	22	0.015
40	7.6	62	0.12	1.55	338	0.0046
77	10.5	207	0.051	2.2	680	0.0032
300	21	1647	0.013	4.9	1900	0.0026

Table III. Dimensions of carbon resistors

Size (W)	length		Carbon slug		lead dia. (mm)
	(mm)	dia. (mm)	length (mm)	dia. (mm)	
1/8	3.7	1.57	3.0	0.79	0.30
1/4	6.4	2.29	5.1	1.32	0.64
1/2	9.5	3.56	7.7	2.26	0.84

$$\tau = 2.2 t^2 / \alpha. \quad (6)$$

If the phenolic is removed from the resistor, then the time constant becomes much faster. For an infinite cylinder subject to a step change in temperature on the surface, the center temperature has a thermal time constant of<sup>18</sup>

$$\tau = 0.256 r^2 / \alpha, \quad (7)$$

where  $r$  is the radius of the cylinder. Table IV lists the calculated internal time constants for the complete resistors ( $\tau_1$ ) and for the resistors with the phenolic removed ( $\tau_2$ ). Both of these time constants neglect end effects. The calculated values for  $\tau_1$  and  $\tau_2$  are shown in Figure 5 as a comparison with the measured values in liquid He and liquid N<sub>2</sub>. The measured values are significantly faster than  $\tau_1$ , which is presumably due to end effects, and because the calculation was for a flat-plate phenolic rather than a hollow cylinder. Nevertheless, the measured time constants are slower than the  $\tau_2$  for carbon cylinders.

We note that from Table IV the 1/8 W resistor with the phenolic removed shows a very fast internal time constant, although this was never measured. For temperature measurements in the  $\mu$ s range, the diameter of the carbon thermometer must be reduced significantly. The carbon fiber which was tested had a fiber diameter of 8  $\mu$ m. Its calculated internal time constant according to Eq (7) is then 0.045  $\mu$ s at 4 K, 0.81  $\mu$ s at 77 K, and 3.2  $\mu$ s at 300 K. The measured values shown in Table I are longer, probably because fibers internal to the bundle were not in good thermal contact with the liquid bath.

Table IV. Calculated internal time constants for carbon resistors

T (K)	1/8 W		1/4 W		1/2 W	
	$\tau_1$ (s)	$\tau_2$ (ms)	$\tau_1$ (s)	$\tau_2$ (ms)	$\tau_1$ (s)	$\tau_2$ (ms)
4	0.057	0.44	0.090	1.2	0.158	3.6
10	0.223	0.77	0.352	2.1	0.620	6.3
40	0.727	3.3	1.15	9.1	2.02	27
77	1.05	7.9	1.65	22	2.90	64
300	1.29	31	2.03	87	3.6	255

So far only the internal time constant has been considered. For sensors which are surrounded by a still gas, the heat transfer coefficient can be so low that the thermal resistance at the boundary dominates the internal thermal resistance. In that case the time constant is given by

$$\tau = C/h\sigma, \quad (8)$$

where  $C$  is the total heat capacity of the thermometer,  $h$  is the heat transfer coefficient between the thermometer and surroundings, and  $\sigma$  is the surface area. For free-convection heat transfer from horizontal cylinders of diameter  $D$ , the Nusselt number,  $Nu = hD/k$ , is a function of the product of  $GrPr$ , where the Grashof number is

$$Gr = \rho^2 \beta g D^3 \Delta T / \mu^2 \quad (9)$$

and the Prandtl number is

$$Pr = c_p \mu / k. \quad (10)$$

In these two equations,  $\rho$  is the fluid density,  $\beta = (1/V)(dv/dT)_p$ ,  $g$  is the acceleration of gravity,  $\Delta T$  is the temperature difference between the surface and the fluid far removed from the cylinder,  $\mu$  is the absolute viscosity,  $c_p$  is the fluid specific heat at constant pressure, and  $k$  is the fluid thermal conductivity. Kreith<sup>18</sup> shows a graph for the functional relationship

$Nu = f(GrPr)$ , from which  $h$  for the carbon resistors was derived.

Table V gives a comparison between the experimental conductance  $K_{exp}$ , the calculated conductance through the phenolic  $K_p$ , and the calculated boundary conductance  $h\sigma$  for the various carbon thermometers in the gas phase. Values for  $K_{exp}$  are only approximate since accurate  $R$  versus  $T$  curves for the thermometers were not determined. Table V shows that at 4.2 K the thermal resistance through the phenolic layer dominates that of the boundary; hence, there should be little difference between time constants with the resistor in the liquid and in the gas. The experimental time constants in Table I show this to be the case at 4.2 K. At 77 K Table V shows the thermal resistance at the boundary dominates, especially in  $N_2$  gas. Experimentally we observe a much higher conductance in  $N_2$  gas, which is due to the heat flow out the leads. Thus, the observed time constants at 77 K in  $N_2$  gas are much faster than the values 32 s, 56 s, and 109 s calculated by Eq (8) for the 1/8 W, 1/4 W, and 1/2 W resistors, respectively.

Table V. Thermal conductances in carbon resistors (mW/K)

Size	4.2 K			77 K			
	$K_{exp}$	$K_p$	$h\sigma$	$K_{exp}$	$K_p$	$h\sigma$	$h\sigma$
$R$ $\mu m$			0.60				
1/8 W	0.38	0.28	2.6	1.7	6.2	1.4	0.13
1/4 W	0.31	0.59	6.0	3.8	13	2.8	0.26
1/2 W	0.80	1.1	12.4	4.9	24	5.2	0.46

The miniature diode thermometer is encapsulated in epoxy and is nearly a sphere 0.5 mm diameter. For the purpose of calculation, we assume the epoxy to have the same thermal properties as the phenolic listed in Table II. For a sphere the internal thermal time constant is<sup>18</sup>

$$\tau = 0.17 r^2/\alpha. \quad (11)$$

Figure 5 shows the calculated time constant for an epoxy sphere at 4.2 K and 77 K. The measured time constant at these temperatures for the miniature diode is somewhat larger, as shown in Figure 5.

The silicon-on-sapphire thermometer is not only one of the fastest thermometers tested, but it also has a calibration which is quite reproducible. The experimental response curve of this thermometer immersed in liquid He is shown in Figure 6. We see that after the initial rise time with a  $\tau$  of 6  $\mu s$ , there is a smaller rise which takes place over a much longer period of time (note the change in scales). This secondary rise is probably due to a small thermal coupling through the leads to the sample holder. The structure in the curve around 4  $\mu s$  is probably a result of electrical noise and the finite sampling time (2  $\mu s$ /point).

The structure of the SOS thermometer is quite simple and the thermal properties are well known, which makes it easy to calculate the internal time constant. First we consider the time required for temperature equilibrium through the thickness of the sapphire; the time constant is given by Eq (6) with  $t = 0.125$  mm. The thermal conductivity<sup>15</sup> and specific heat<sup>19,20</sup> of sapphire of density 3.97 g/cm<sup>3</sup> are used to calculate  $\alpha$  as a function of temperature. The calculated time constant  $\tau_t$  for equilibrium through the thickness of the sapphire is shown in Figure 7. This time constant would be characteristic of the SOS thermometer if the active thermometer element covered the entire sapphire substrate. However, with our self-heating method of measuring  $\tau$ , heat must diffuse through the sapphire from the location of the thermometer element to the edges of the substrate. This time constant  $\tau_w$  is much longer than  $\tau_t$  and is calculated from Eq (6) by using an average dimension of 4 mm for  $t$ . The temperature dependence of  $\tau_w$  is also shown in Figure 7 along with the experimental results at 4.2 and 77 K. The observed

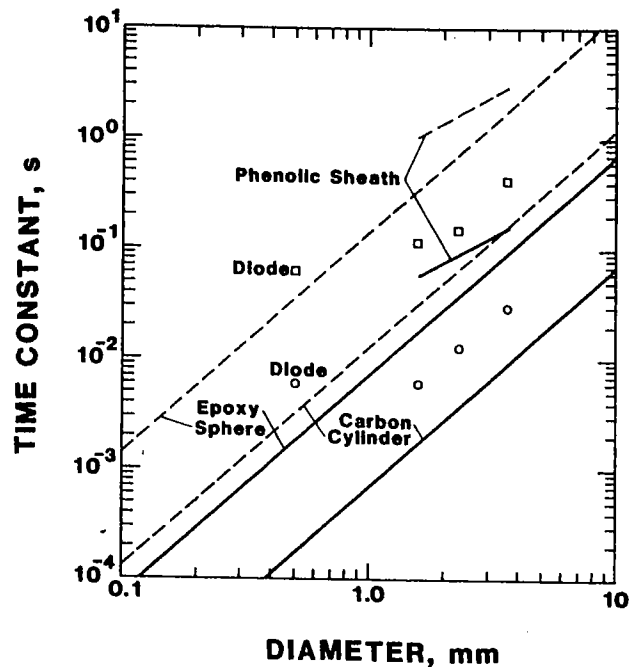


Figure 5. The size dependence of various calculated and measured time constants. The solid lines are calculated values at 4.2 K and the dash lines are for 77 K. The circles and squares are experimental data at 4.2 K and 77 K respectively. The diode referred to is the miniature diode.

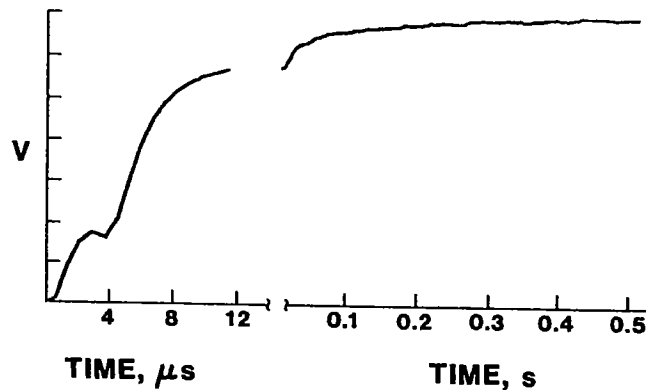


Figure 6. Response curve of SOS thermometer in liquid He. Note change in time scale. Vertical axis calibrated in arbitrary units.

time constants for liquid contact are somewhat faster than  $\tau_w$  because the high heat transfer coefficient to the liquid cryogen means that the temperature gradient in the sapphire extends only a short distance from the thermometer element and the remote edges of the substrate remain nearly at the same temperature as the liquid bath.

It is important to point out that if this thermometer were used to sense a step change in temperature of its surroundings, it would respond with the time constant of  $\tau_t$  since the heat transfer would be uniform over the whole surface area instead of localized to the thermometer element. As seen in Figure 7, at low temperatures this thermometer could be extremely fast. In practice the finite boundary conductance usually limits the time in which the thermometer can respond to a change in temperature of its surroundings. Figure 7

The authors wish to thank Warren Pierce of Lake Shore Cryotronics, Inc. for supplying the miniature silicon diode thermometers and Steve Early of Stanford University for supplying the silicon-on-sapphire thermometers used in this work. They also thank Jim Herbert of Allen-Bradley Electronics Division for supplying dimensional information concerning carbon-composition resistors.

## REFERENCES

- a) Contribution of the National Bureau of Standards, not subject to copyright.
- b) Work partially supported by Flight Dynamics Laboratory, Wright-Patterson Air Force Base, Ohio.
1. R. M. Carroll and R. L. Shepard, "Measurement of the transient response of thermocouple and resistance thermometers using in-situ method," Oak Ridge National Laboratory Report ORNL-TM-4573 (1977).
2. B. Hague and T. R. Foord, *Alternating Current Bridge Methods*, Pittman, New York, NY (1971) pp. 87-90.
3. T. W. Kerlin, H. M. Hashemian, and K. M. Peterson, *ISA Trans.* **20**, 65 (1981).
4. T. W. Kerlin, R. L. Shepard, H. M. Hashemian, and K. M. Peterson, *Temperature, Its Measurement and Control in Science and Industry* (American Institute of Physics, NY, 1982), Vol. V. (To be published in this volume). Hereafter referred to as *Temperature*.
5. T. W. Kerlin, L. F. Miller, H. M. Hashemian, and W. P. Poore, "In-situ response testing of platinum RTDs," Electric Power Research Institute Report NP-834 (Vol. 1) prepared by the Nuclear Engineering Department of the University of Tennessee (1978).
5. R. Radebaugh, J. D. Siegwarth, W. N. Lawless, and A. J. Morrow, "Electrocaloric Refrigeration for Superconductors," National Bureau of Standards Report NBSIR76-847 (1977) p. 33.
7. E. G. Brentari and R. V. Smith, *Adv. Cryog. Eng.* **10**, 325 (1965).
8. H. Weinstock and J. Parpia, *Temperature*, Vol. 4, Part 2 (1972) p. 785.
9. R. C. Pandorf, C. Y. Chen, and J. G. Daunt, *Cryogenics* **2**, 239 (1962).
10. G. Halverson and D. A. Johns, *Temperature*, Vol. 4, Part 2 (1972) p. 803.
11. S. R. Early, F. Hellman, J. Marshall, and T. H. Geballe, *Physica* **107B**, 327 (1981).
12. S. R. Early, "Small sample calorimetry at low temperatures," Doctoral dissertation, Stanford University (1981) pp. 63-87.
13. J. S. Blakemore, *Temperature*, Vol. 4, Part 2 (1972) p. 827.
14. V. J. Johnson, "A compendium of the properties of materials at low temperature," Wright Air Development Division Technical Report 60-56, Part II (1960).
15. G. E. Childs, L. J. Ericks, and R. L. Powell, National Bureau of Standards Monograph 131 (1973).
16. T. A. Scott, J. DeBruin, M. M. Giles, and C. Terry, *J. Appl. Phys.* **44**, 1212 (1973). (The specific heat per unit volume of phenolic is not known, but the values of nylon were assumed to be similar.)
17. M. Jakob, *Heat Transfer*, Vol 1, John Wiley and Sons, New York (1949) p. 316.
18. F. Kreith, *Principles of Heat Transfer*, International Textbook Company, Scranton, NY (1960) p. 305.
19. R. Q. Fugate and C. A. Swenson, *J. Appl. Phys.* **40**, 3034 (1969).
20. G. T. Furukawa, T. B. Douglas, R. E. McCoskey, and D. C. Ginnings, *J. Res. Nat. Bur. Stand.* **57**, 67 (1956).
21. R. Radebaugh, *Rev. Sci. Instrum.* **48**, 93 (1977).

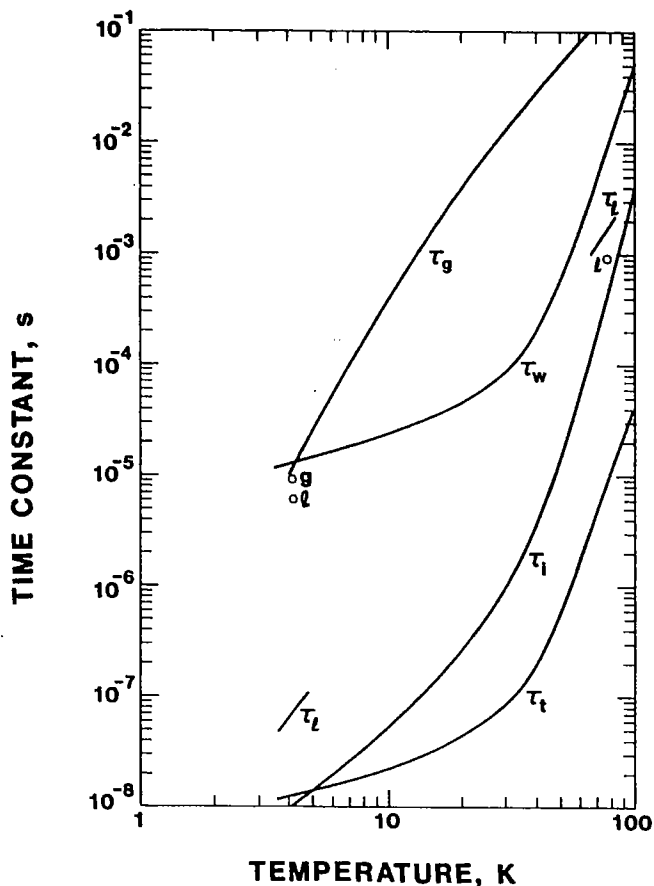


Figure 7. The temperature dependence of time constants for the SOS thermometer. The  $x$  and  $o$  next to the experimental points indicate whether the thermometer was in liquid or gas. The various calculated time constants are discussed in the text.

shows the time constants for the thermometer if the heat transfer is limited by the boundary conductance for the case of still He gas ( $\tau_g$ ), liquid He or liquid  $N_2$  ( $\tau_l$ ), and an indium solder joint<sup>19</sup> on the back side of the substrate ( $\tau_i$ ). These conductance-limited time constants are calculated by using Eq (8). We see that boundary conductances are never high enough to permit the thermometer to respond as fast as  $\tau_t$ . The only exception would be for the case of incident radiation on the thermometer, as in a bolometer. The high boundary conductance in still  $N_2$  gas leads to a relatively long time constant for that situation as shown in Table I.

## CONCLUSIONS

The time constants given here for various cryogenic thermometers can be used as rough guides to the selection of a proper thermometer for the measurement of transient temperatures. Accurate values for a particular thermometer are best determined by an *in-situ* measurement using the self-heating method described here. In general, the smaller the thermometer, the faster it will respond. Construction materials for the thermometer can have a large effect on the response times. In particular, the high thermal diffusivity of silicon and sapphire at low temperatures leads to very fast time constants for the silicon-on-sapphire thermometer. At 4 K, time constants of less than 1  $\mu$ s are possible, which is much faster than room temperature thermometers. The effect of the mounting arrangement must be considered in response times of thermometers if accurate measurements are to be made.